ACS Catalysis

Research Article

pubs.acs.org/acscatalysis

Bifunctional Adsorbent-Catalytic Nanoparticles for the Refining of Renewable Feedstocks

Kapil Kandel,[†,‡] Conerd Frederickson,[†] Erica A. Smith,[‡] Young-Jin Lee,[†,‡] and Igor I. Slowing*[,†,‡]

[†]U. S. Department of Energy, Ames Laboratory, Ames, Iowa 50011-3020, United States

[‡]Department of Chemistry, Iowa State University, Ames, Iowa 50011-3111, United States

Supporting Information

ABSTRACT: A hybrid adsorbent-catalytic nanostructured material consisting of aminopropyl groups and nickel nanoparticles immobilized in mesoporous silica nanoparticles (AP-Ni-MSN) was employed to selectively capture free fatty acids (FFAs) and convert them into saturated hydrocarbons. The working principle of these sorbent-catalytic particles was initially tested in the hydrogenation of oleic acid. Besides providing selectivity for the capture of FFAs, the adsorbent groups also affected the selectivity of the hydrogenation reaction, shifting the chemistry from hydrocracking-based (Ni) to hydrotreating-based and improving the carbon economy of the process. This approach was ultimately evaluated by the selective sequestration of FFAs from crude microalgal oil and their subsequent conversion into liquid hydrocarbons, demonstrating the suitability of this design for the refinery of renewable feedstocks.

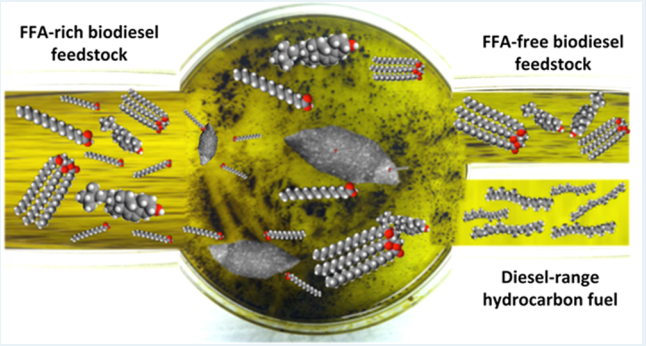

KEYWORDS: *mesoporous silica nanoparticles, hydrotreatment, biorenewable feedstock, microalgae, biofuel*

INTRODUCTION

The refining of crude biodiesel to remove oxygenated impurities is required to meet the specifications for transportation fuels.[1−3] Free fatty acids (FFAs) are the most prominent oxygenated impurities in biodiesel feedstocks and are undesirable because they react with the basic catalyst used for transesterification to form soap.[4] The FFA content in the feedstock must be lower than 0.5 wt % and thus requires the use of highly refined oils.[1,5] We recently demonstrated that aminopropyl functionalized mesoporous silica nanoparticles (AP-MSNs) selectively sequester FFAs from crude algal oil to meet the specifications of feedstocks for biodiesel.[6,7] The sequestered FFAs could still be converted into biodiesel by acid catalyzed esterification with methanol.

FFAs can also be converted into fuel by hydrogenation. The products of the reaction are liquid hydrocarbons, which are more similar to petroleum-based fuels.[8−10] Because they lack oxygen, hydrocarbons are more stable and have higher energy density than FFAs or biodiesel.[10,11] Furthermore, hydrogenation also eliminates unsaturations common in algal or plant oils, increasing their cetane number.[12] The hydrogenation of FFAs can be performed using supported noble metal catalysts such as Pd and Pt.[13−20] However, the high price of these metals demands more economical alternatives. While supported Ni is fairly active in the hydrogenation of methyl esters of FFA, it has poor selectivity, favoring cracking over hydrodeoxygenation to give broad hydrocarbon distributions.[21] It is well-known that modifying the composition of catalysts changes their activity and selectivity.[22−26] In this sense, Ni, Co, and Mo sulfides supported on metal oxides have been evaluated for the deoxygenation of bio-oils.[27−29] Nevertheless, gradual desulfurization of these catalysts leads to a loss of activity and contamination of the fuel with the leached sulfides.[28,30,31] Using nickel phosphide instead of the sulfide avoids these problems and preserves carbon economy by increasing the selectivity for hydrodeoxygenation and decarbonylation over cracking.[21]

The activity and selectivity of heterogeneous catalysts can also be improved using auxiliary groups.[32,33] In this regard, it is particularly attractive to use groups that can selectively adsorb reactants or byproducts to control the course of catalytic processes. For example, Sano and co-workers observed recently that the photodegradation of formic acid and phenol by TiO_2 was dramatically improved after the addition of amine functionalized mesoporous silica nanomaterials. The amines facilitated the process by adsorbing the CO_2 evolved during the reaction.[34] Lercher and co-workers have applied the combination between adsorbents and catalysts to the hydrogenation of FFAs.[35,36] In a recent work, they supported Ni on ZrO_2 and observed efficient conversion of FFAs to hydrocarbons.[35] They showed that adsorption of the acids to oxygen vacancies in ZrO_2 led to a

Received: July 2, 2013
Published: October 15, 2013

Scheme 1. Representation of the Integrated Adsorbent-Catalytic System

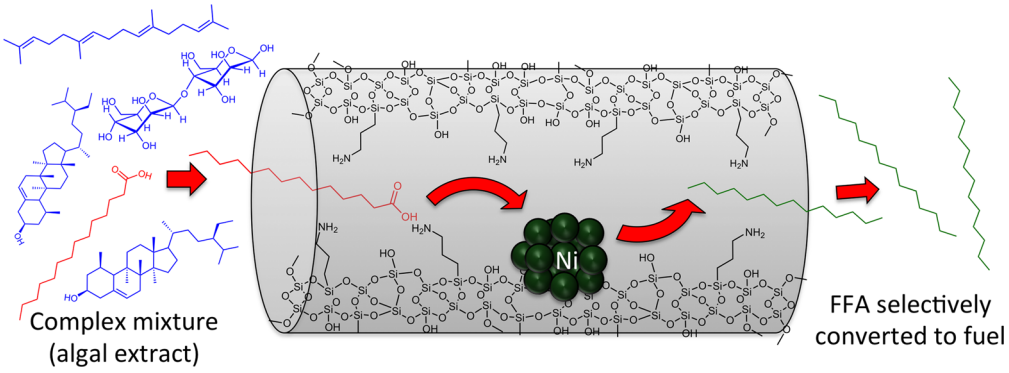

parallel reaction involving α-hydrogen abstraction to ketene that was later reduced and decarbonylated by nickel. Thus, the product was obtained simultaneously by the direct reduction on nickel, and through the ZrO_2 mediated reaction, both processes giving high selectivity for decarbonylation.

Since bio-oils are complex mixtures containing raw materials for diverse applications, a catalyst for hydrogenation could benefit from the incorporation of an auxiliary group capable of selectively sequestering their FFA substrates. This group would feed the catalyst with FFAs, leaving all other substances in the mixture unmodified and available for downstream processing. On the basis of our previous observation of the selectivity of AP-MSN for sequestering FFAs from algal oils,[6,7] we decided to use amines as auxiliary groups for the Ni catalyzed hydrogenation of FFAs. In our design, amine groups within a mesoporous support would capture the FFAs and control their access to the catalyst (Scheme 1). We first evaluated individually the adsorptive and catalytic properties of the material using oleic acid as a general model of FFAs; then we evaluated the combined adsorption-catalytic process on oleic acid, and finally we applied this integrated approach to the conversion of crude microalgal oil into liquid hydrocarbons.

MATERIALS AND METHODS

Materials. Pluronic P104 was kindly provided by BASF. Tetramethyl orthosilicate (TMOS) was purchased from Sigma-Aldrich. 3-Aminopropyl trimethoxysilane (APTMS) was purchased from Gelest. Nickel nitrate hexahydrate $[Ni(NO_3)_2{\cdot}6H_2O]$ and ammonium phosphate $[(NH_4)_2HPO_4]$ were purchased from Fisher Scientific.

Synthesis of Mesoporous Silica Nanoparticles (MSN). MSN was prepared using a nonionic block copolymer Pluronic P104 surfactant.[37] For a typical synthesis, P104 (7.0 g) was added to HCl (273.0 g, 1.6 M). After stirring for 1 h at 56 °C, tetramethylorthosilicate (TMOS, 10.64 g) was added and stirred for an additional 24 h. The resulting mixture was further post hydrothermally treated for 24 h at 150 °C in a Teflon-lined autoclave. Upon cooling to room temperature, the white solid was collected by filtration, washed with copious amounts of methanol, and dried in the air. To remove the surfactant P104, the MSN material was heated at a ramp rate of 1.5 °C min^{-1} to calcine at 550 °C for 6 h.

Synthesis of Nickel Nanoparticles in the Pores of MSN (Ni-MSN). MSN was mixed with water and stirred at room temperature in order to rehydrate and regenerate the silanol groups, followed by filtration and drying. $Ni(NO_3)_2{\cdot}6H_2O$ (0.55 mmol, 0.16 g) was completely dissolved in water (0.48 mL). To this solution, the rehydrated MSN (0.4 g) was added and mixed. The solid mixture was calcined in the air at a heating rate of 2 °C min^{-1} to 500 °C and maintained at that temperature for 6 h followed by reduction at 450 °C for 5 h in a constant flow of H_2 (0.5 mL/s).

Synthesis of Organofunctionalized Ni-MSN. Amine functionalized materials were prepared by grafting APTMS (2 mmol, 0.36 g) to the surface of Ni-MSN (1.0 g) in refluxing toluene (100 mL) for 24 h. The resulting solid was filtered, washed with methanol, and dried under a vacuum for 24 h. A material with lower loading of amines was prepared using 1 mmol (0.18 g) of APTMS, and a material grafted with hexyl groups was prepared using hexyl-trimethoxysilane (2 mmol, 0.41 g) instead of APTMS.

Characterization. Surface analysis of the catalyst was performed by nitrogen sorption isotherms in a Micromeritics Tristar surface area and porosity analyzer. The surface areas were calculated by the Brunauer–Emmett–Teller (BET) method, and the pore size distribution was calculated by the Barrett–Joyner–Halenda (BJH) method. The small angle powder X-ray diffraction patterns were obtained with a Rigaku Ultima IV diffractometer using Cu target at 40 kV and 44 mA. Cu Kβ was removed using a monochromator. For transmission electron microscopy measurements, the powder was suspended in methanol by sonication for 15 min. A single drop of this suspension was placed on a lacey carbon coated copper TEM grid and dried in the air. The TEM examination was completed on a Tecnai G2 F20 electron microscope operated at 200 kV. Fourier transform infrared (FT-IR) spectra were recorded on Nicolet Nexus 470. PerkinElmer ICP-MS was used to measure Ni loading, and Agilent GC-MS was used to measure reaction products. Aminopropyl group loading was measured by elemental analysis in a PerkinElmer 2100 Series II CHN/S Analyzer, using acetanilide as a standard and combustion and reduction at 925 and 640 °C.

General Procedure for One-Pot Batch Reaction. All catalytic reactions were performed in a batch reactor (Parr Instruments). In a typical experiment, the catalyst (10 mg) and oleic acid solution in hexanes (1 mM, 10 mL) were added to the reactor. The reactor was purged with H_2 at ambient temperature and was finally pressurized by H_2 to 30 bar. The reaction was then carried out at 290 °C for 6 h with a constant stir rate. The reaction was allowed to cool to room temperature, and the products were subjected to esterification of the remaining oleic acid to its methyl ester for analysis by GC-MS. In order to derivatize, the hexanes were removed

dx.doi.org/10.1021/cs4008039 | ACS Catal. 2013, 3, 2750–2758

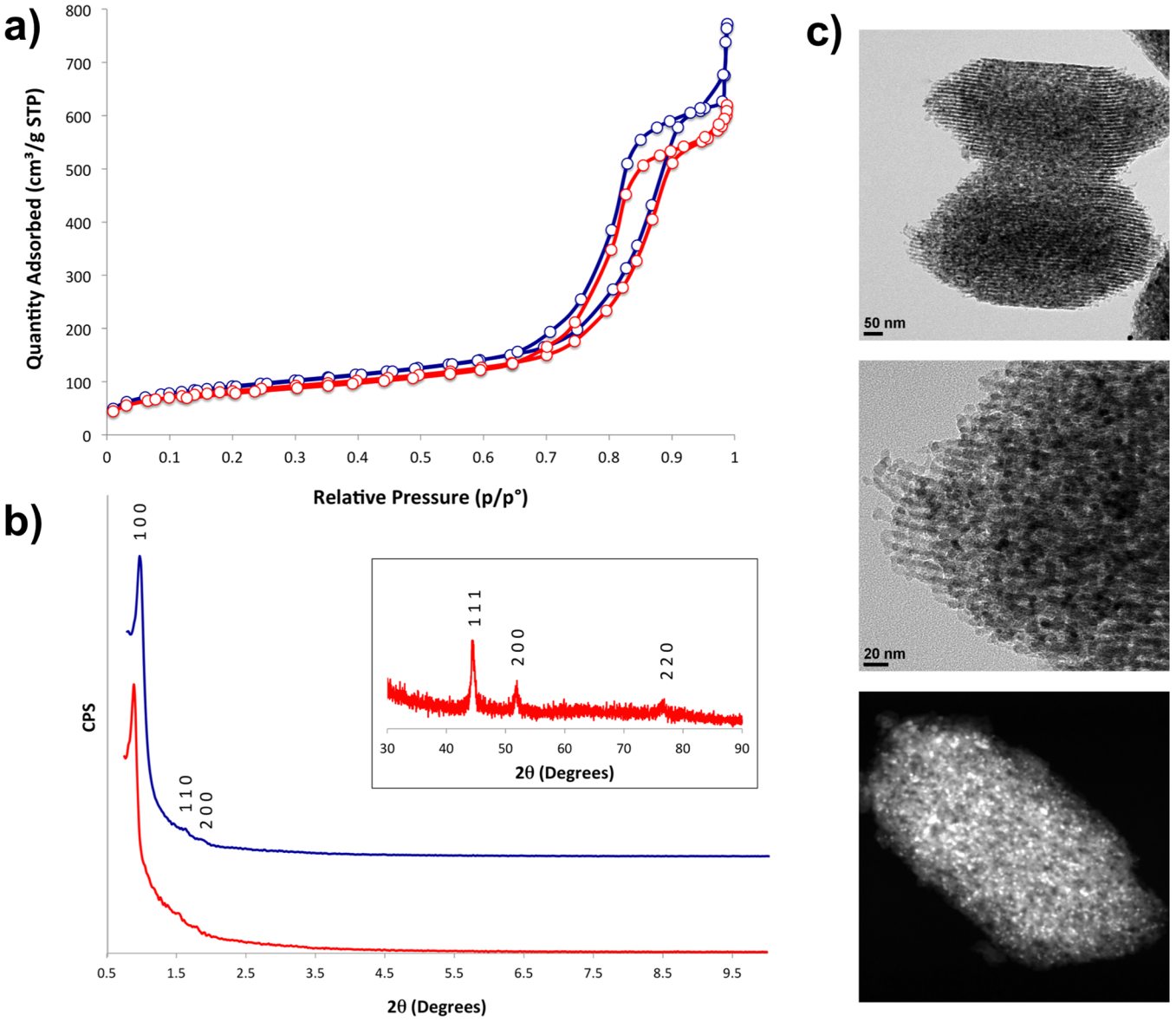

Figure 1. (a) Nitrogen sorption isotherms. (b) Wide (inset) and small angle XRD patterns of MSN support (blue) and Ni-MSN (red). (c) TEM (top and center) and STEM (bottom) images of Ni-MSN. The dark spots in the TEMs and the bright spots in the STEM correspond to Ni nanoparticles.

under reduced pressure followed by the addition of a solution of HCl in methanol (1 M, 2 mL). The mixture was stirred for 1 h at 80 °C. After cooling to room temperature, NaCl (1%, 1 mL) was added to the reaction mixture. The ester of oleic acid was then extracted with hexanes (3 × 3 mL) and analyzed by GC-MS using methyl nonadecanoate as an internal standard.

General Procedure for Sequential Batch Reaction. In a typical two-step process, the catalyst (10 mg) was added to a test tube containing the oleic acid solution in hexanes (1 mM, 10 mL) and mixed for 6 h, and then the suspension was centrifuged. The amount sequestered was calculated by measuring the oleic acid remaining in the supernatant. To convert the sequestered oleic acid to hydrocarbons, the catalyst remaining after centrifugation was mixed with 10 mL of hexanes, and the mixture was loaded to the reactor. After purging with H_2, the reaction mixture was pressurized by H_2 to 30 bar and kept at 290 °C for 6 h with constant stirring. The reaction was allowed to cool to room temperature, and the liquid samples were analyzed by GC-MS using methyl nonadecanoate as internal standard.

Analysis of Lipids in Algal Extracts. The APCI-HRMS analysis of the algal extracts was done on a linear-trap-orbitrap hybrid mass spectrometer (LTQ-Orbitrap Discovery, Thermo Scientific, San Jose, CA, USA). The oil, before and after mixing with the AP-Ni-MSN, was manually injected with a divert valve at 0.01% (v/v) with 50% methanol in toluene. Further details about the APCI-HRMS conditions can be found elsewhere.[7]

RESULTS AND DISCUSSION

Synthesis and Catalytic Activity of Ni-MSN. The mesoporous silica nanoparticle (MSN) support was prepared according to a previously published method[37] and consisted of elongated particles about 650 × 400 nm in size. XRD analysis indicated hexagonal arrangement of pores typical of SBA-15

dx.doi.org/10.1021/cs4008039 | ACS Catal. 2013, 3, 2750−2758

Table 1. Summary of Textural Properties of Catalysts

sample	surface area (m^2/g)	pore volume (cm^3/g)	pore size (nm)	Ni loading (wt %)
MSN	331	0.97	11.1	
Ni-MSN	298	0.88	11.0	6.9
AP-Ni-MSN	209	0.60	8.9	6.5

type materials,[38] and nitrogen sorption analysis revealed a type IV isotherm characteristic of mesoporous materials (Figure 1a). BET and BJH calculations indicated a large surface area and a sharp pore size distribution centered at 11.1 nm (Table 1). The catalytic Ni nanoparticles were prepared by impregnation of the support with aqueous $Ni(NO_3)_2 \cdot 6H_2O$, followed by calcination in the air and reduction under a H_2 stream at 450 °C. The resulting Ni-MSN material had 6.9 wt % Ni, with an XRD pattern indicating crystalline elemental nickel exclusively in the fcc phase (JCPDS 04-0850, Figure 1b).[39] TEM, STEM, and EDX measurements suggested that most of the Ni nanoparticles formed within the pores of MSN (Figure 1c). The structure of the support was not affected by the growth of the Ni nanoparticles, as the small angle XRD patterns still displayed the reflections corresponding to a hexagonal array of pores. The material retained the type IV nitrogen sorption isotherm, confirming it was still mesoporous (Figure 1).[40] As expected, the surface area and pore volume of the parent MSN decreased upon formation of Ni nanoparticles (each by 10%); however the pore size remained almost constant at 11.0 nm (Table 1). These results are consistent with the formation of the particles inside of the pores.[41]

Oleic acid was used as a model to evaluate the catalytic activity of Ni-MSN in the hydrogenation of FFAs. The reaction was performed by adding 10 mg of catalyst to 10 mL of 1 mM oleic acid solution in hexane and heating at 290 °C under 30 bar H_2 for 6 h in batch mode. The selectivity of the reaction was defined according to three main types of hydrocarbon products: hydrocracking ($<C_{17}$), decarbonylation (C_{17}), and hydrodeoxygenation (C_{18}) (Scheme 2). The reaction proceeded with full conversion using Ni-MSN as a catalyst. Consistent with the results of Serrano et al. on methyl esters of FFAs, our Ni-MSN catalyst favored cracking (72%) over decarbonylation (25%) and hydrodeoxygenation (3%) (Figure 2).[21]

Adsorptive Properties of Aminopropyl Modified Ni-MSN. The current technologies for separation and purification of organic acids involve extraction and distillation using organic solvents and supercritical fluids, which makes the process expensive and energy intensive.[42,43] Recently, we have shown the selective sequestration of free fatty acids from complex mixtures using 3-aminopropyl functionalized MSN (AP-MSN).[6] Therefore, to incorporate adsorption and catalysis into a single unit, Ni-MSN was grafted with 3-aminopropyl trimethoxysilane. While the resulting AP-Ni-MSN material was still mesoporous (Figure S1), a decrease in pore volume, pore size and surface area was observed after functionalization (Table 1). This drop in surface properties has been previously observed upon AP grafting of mesoporous silicas.[44−46] Elemental analysis indicated a load

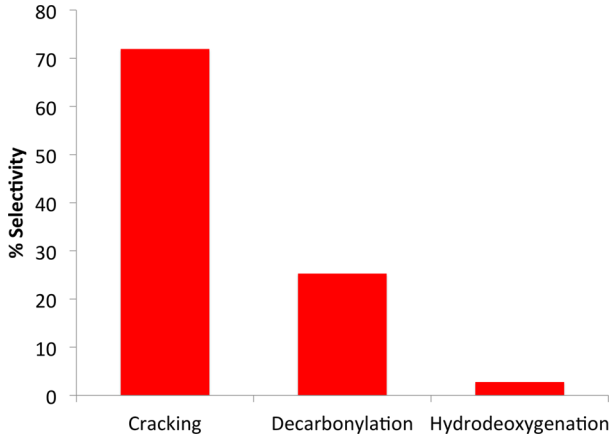

Figure 2. Product distribution in the hydrogenation of oleic acid catalyzed by Ni-MSN (10 mL of 1 mM oleic acid in hexane, 10 mg of Ni-MSN, 290 °C, 30 bar H_2, 6 h).

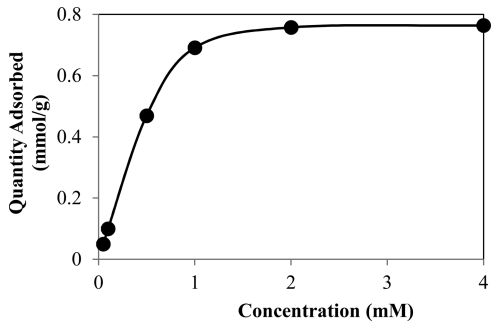

Figure 3. Adsorption isotherm of oleic acid on AP-Ni-MSN.

Scheme 2. Possible Reaction Routes

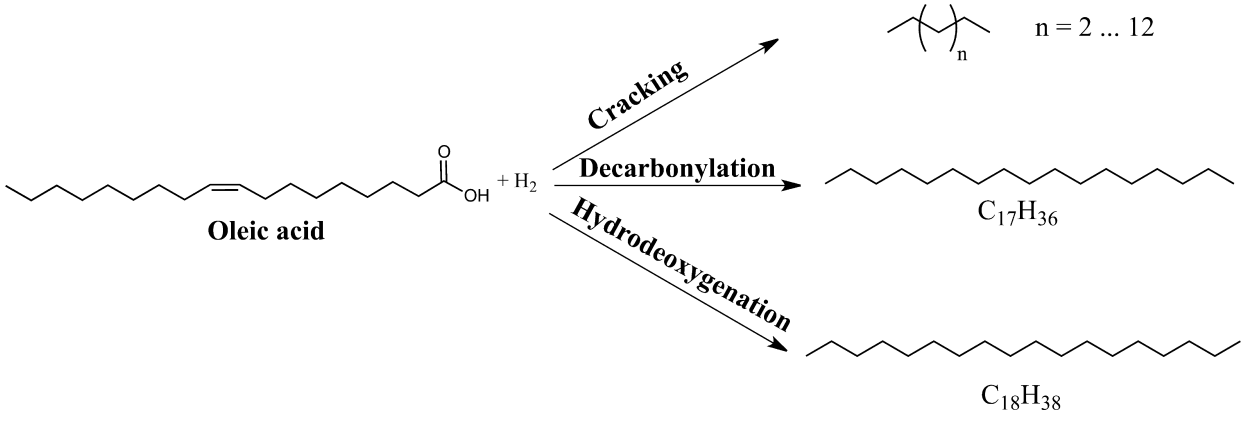

dx.doi.org/10.1021/cs4008039 | ACS Catal. 2013, 3, 2750−2758

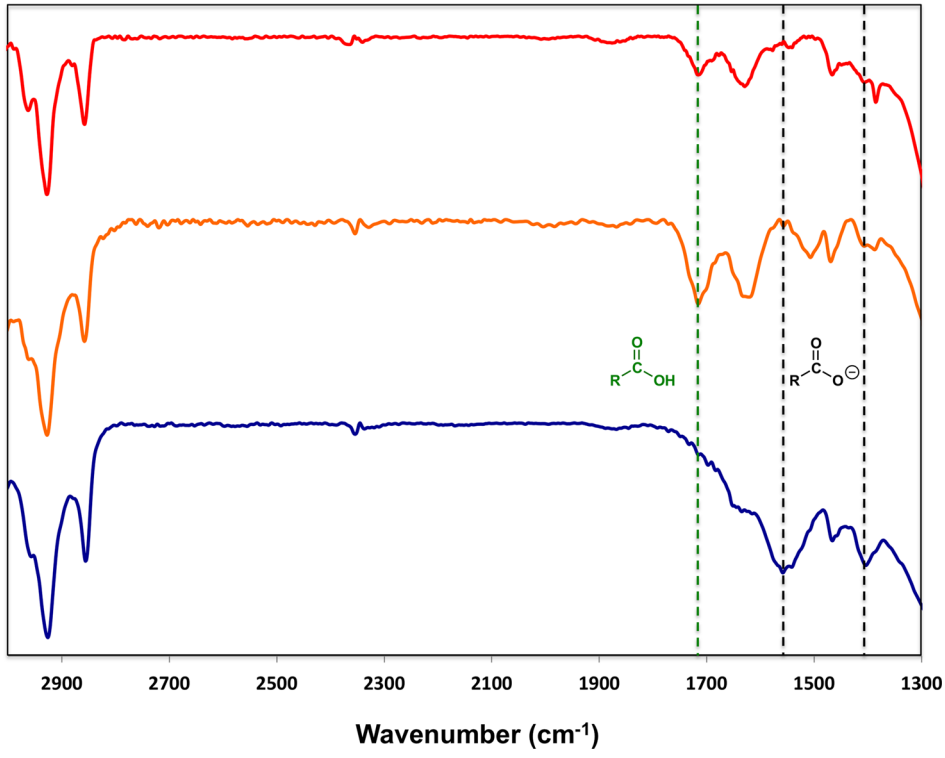

Figure 4. FTIR spectra of Ni-MSN (red), AP-MSN (orange), and AP-Ni-MSN (blue) following adsorption of oleic acid. Discontinuous lines show the absorption by the acid (green, 1710 cm^{-1}) and the carboxylate ion (black, 1562 cm^{-1} and 1407 cm^{-1}).

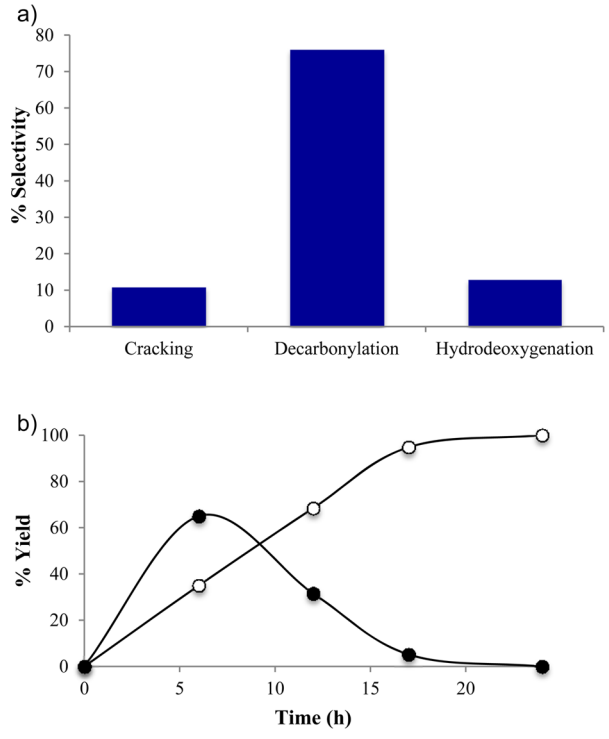

Figure 5. (a) Product selectivity in the hydrotreatment of oleic acid with AP-Ni-MSN and (b) kinetics of stearic acid (black circles) and total hydrocarbon (white circles) formation (10 mL 10 mM oleic acid in hexane, 10 mg AP-Ni-MSN, 290 °C, 30 bar H_2).

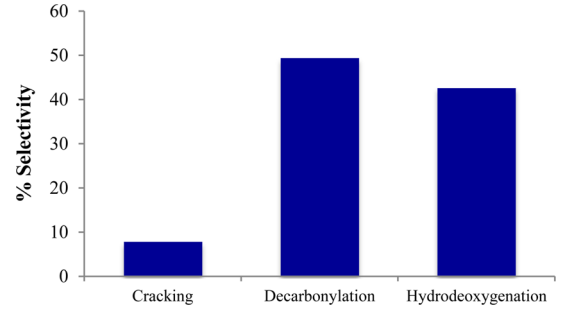

Figure 6. Product distribution observed following the sequential sequestration catalysis of oleic acid by AP-Ni-MSN.

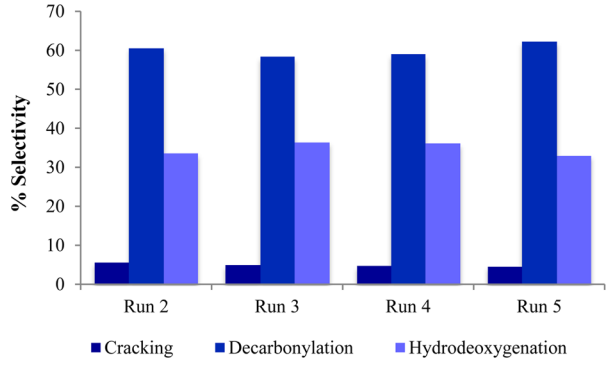

Figure 7. Product distribution of successive hydrotreatment reactions of oleic acid catalyzed by AP-Ni-MSN.

of 1.4 mmol AP groups per gram, suggesting the formation of a dense layer of amines on the material, which is consistent with the decrease in surface properties of Ni-MSN.

To examine the capacity of the material to sequester FFAs, AP-Ni-MSN was added to solutions of oleic acid in hexane, and the mixtures were shaken at room temperature for 6 h. Fitting the adsorption isotherm (Figure 3) to the Langmuir

dx.doi.org/10.1021/cs4008039 | ACS Catal. 2013, 3, 2750−2758

model gave a maximum adsorption of 0.76 mmol oleic acid per gram of material, corresponding to a 0.54:1 molar ratio of sequestered oleic acid to amine groups. This result is in a sharp contrast with our previous report in which the maximum adsorption of FFA to AP-MSN with a similar amine load and surface properties gave a 1:1 molar ratio. The limited binding of FFAs by AP-Ni-MSN in this work suggests that a fraction of the amines are unavailable, possibly due to a strong interaction with the surface of Ni. A comparison of FTIR spectra of AP-Ni-MSN with those of AP-MSN supports this hypothesis (Figure S2). In AP-MSN, the absorption due to scissor vibrations of amine (1621 cm^{-1}) overlaps with the broad scissoring band of adsorbed water (1630 cm^{-1}). However, in AP-Ni-MSN the same vibration is downshifted to 1587 cm^{-1}, very likely due to ligand binding to the surface of the nickel, similarly to previous reports on the interaction of amines with various nanoparticles.[47,48] In the absence of an aminopropyl group, Ni-MSN adsorbs only a maximum of 0.15 mmol/g of oleic acid.

The sequestration of oleic acid by AP-Ni-MSN was confirmed by the sharp C−H stretching bands at 2926 cm^{-1} and 2850 cm^{-1} and the asymmetric and symmetric carboxylate vibrations at 1562 cm^{-1} and 1407 cm^{-1}, respectively (Figure 4). Interestingly, while the FTIR analysis indicated that the oleic acid was adsorbed to AP-Ni-MSN exclusively as a carboxylate ion, the adsorption of oleic acid to Ni-MSN and to AP-MSN showed only the C═O stretching band at 1710 cm^{-1}, indicative of nondissociated carboxylic acid.

Catalytic Properties of AP-Ni-MSN. The presence of amine groups in the material led to a dramatic change in the catalytic hydrogenation of oleic acid (Figure 5a). The AP-Ni-MSN catalyzed reaction showed a sharp decrease in the selectivity for cracking (from 72% to 11%) compared to Ni-MSN. While decarbonylation to heptadecane was the major product of the reaction (76% selectivity), the selectivity for the hydrodeoxygenation to octadecane increased four times (from 3 to 13%), improving the carbon economy of the reaction. Thus, the incorporation of amines into the material turned our initial hydrocracking catalyst into a hydrotreating catalyst. The amine groups also reduced the activity of the catalyst: while the conversion of the starting oleic acid with AP-Ni-MSN after 6 h was 100%, the total hydrocarbon yield was only 72% with the remaining 28% being stearic acid. Increasing 10-fold the concentration of the oleic acid substrate gave also full conversion in 6 h, but the yield of hydrocarbons was limited to 35%, and deoxygenation of the intermediate stearic acid was completed only after 24 h (Figure 5b).

The changes in product distribution were proportional to the amount of amine introduced into AP-Ni-MSN (Figure S3). The selectivity for cracking decreased from 72% in Ni-MSN to 14% in AP-Ni-MSN with 0.4 mmol/g of amine and further to 11% in AP-Ni-MSN with 1.4 mmol/g of amine. Conversely, the selectivity for hydrodeoxygenation increased from 3% to 7% to 13% with Ni-MSN, AP-Ni-MSN (0.4 mmol/g), and AP-Ni-MSN (1.4 mmol/g), respectively. This demonstrated further the impact of the organic groups in controlling the course of the reaction.

Interestingly, performing the reaction using a physical mixture of AP-MSN sorbent and Ni-MSN catalyst led to only 9% hydrocarbon yield compared to the 72% of hydrocarbons obtained using the hybrid AP-Ni-MSN as a catalyst. This result further confirmed the importance of having the amine groups located close to the catalytic sites: while in AP-Ni-MSN the amine groups increased the local concentration of the substrate in the immediacy of the catalytic sites, in the mixed experiment the amine groups of AP-MSN prevented the oleic acid from transferring to the particles containing the catalyst (Ni-MSN). It is remarkable that the interaction between the amine groups and the acid was strong enough to prevent interparticle migration of the substrate even at the high temperatures of the reaction.

Evaluation of the Sequestration-Catalysis Approach. Next, we considered that if the FFA was adsorbed and allowed to accumulate in the pores of AP-Ni-MSN before performing the hydrogenation, the conditions should be significantly different than in the single-pot adsorption-catalysis process described above. To test this hypothesis, the AP-Ni-MSN material was first suspended in a solution of oleic acid in hexane and equilibrated for 6 h at room temperature and atmospheric pressure in a mechanical shaker. The catalyst was then separated by centrifugation, resuspended in hexane, and subjected to hydrogenation under the previously described conditions.

Surprisingly, the selectivity for hydrodeoxygenation (C_{18}) increased by more than 3-fold (43%, Figure 6) compared to that of the one-pot process (13%, Figure 4). The fraction of cracking remained very similar to the one in the single-pot procedure (8% sequential versus 11% one-pot); therefore, the increase in hydrodeoxygenation took place mainly at the expense of the decarbonylation (49% sequential versus 76% one-pot). This remarkable increase in the carbon economy of the reaction was likely caused by saturation of the pores with the preloaded oleate. The small volume remaining in the pores after adsorption could restrict the access of atoms other than the carboxylate oxygens to the surface of the Ni nanoparticles.

Recycling of AP-Ni-MSN. A major concern of introducing amine modifiers to the Ni-MSN system is that Ni is also a catalyst for hydrodenitrogenation reactions.[49,50] However, tethering the amines to the MSN surface may provide a way to prevent or minimize their direct contact with Ni and the consequent loss of nitrogen. As mentioned above, the fact that only 0.76 mmol of oleic acid could be adsorbed by 1 g of material suggested that a fraction of the amines, presumably 0.64 out of 1.4 mmol/g, were directly interacting with Ni. Elemental analysis of the used catalyst showed that indeed 0.6 mmol of nitrogen/g was lost during the reaction. Consistently, the FFA adsorption capacity of the material decreased to about 50% of the original after the reaction. No loss in carbon was observed after reaction, suggesting the loss of nitrogen was a hydrodenitrogenation process.

While the sequestration capacity of the material depends on the presence of the amine groups, the catalytic activity is a function of the Ni nanoparticles. Thus, recycling of the catalyst up to five times led always to 100% conversion over 6 h of reaction. Despite the partial loss of amine groups, the hydrocarbon selectivity of the reaction continued to favor decarbonylation and hydrodeoxygenation over cracking, with distributions similar to those observed for the sequential sequestration-catalysis procedure (Figure 7). This observation suggested that hydrocarbon distribution was affected by the presence of organic groups in the material regardless of their chemical functionality. To further test this possibility, we prepared a new Ni-MSN material grafted with hexyl groups (hexyl-Ni-MSN) and used it as a catalyst for the hydro-

dx.doi.org/10.1021/cs4008039 | ACS Catal. 2013, 3, 2750−2758

genation of oleic acid. The hydrocarbon yield was significantly lower than that obtained with AP-Ni-MSN (29.5%), very likely due to the lack of FFA sequestration capacity of the hexyl groups. However, the selectivity still favored decarbonylation and hydrodeoxygenation over cracking (20% cracking, 68% decarbonylation, and 12% hydrodeoxygenation). This confirmed that the decrease in cracking was not the result of specific interactions between the amine and the catalytic nanoparticles but a nonspecific effect of the organic moieties. A similar decrease in the cracking activity of Ni nanoparticles has been previously observed during the high-temperature deposition of coke within the pores of the support.[51] Thus, the effect we observed could be a steric hindrance caused by the accumulation of organics in the pores, which would limit the diffusion of reactants to the catalytic centers. Indeed, plotting the pore volumes of the materials used in this work against the corresponding yields of each type of product revealed a direct correlation for cracking (r^2 = 0.929) and an inverse correlation for decarbonylation (r^2 = 0.951), indicating that smaller pore volumes favor decarbonylation over cracking (Figure S4). Further work is underway in our laboratories to fully establish the detailed mechanism of the enhanced selectivity.

While the observed effect on product selectivity seems to be independent of the nature of the organic groups, only the amines are able to selectively sequester FFAs, which is a key property for the application of this system to the refining of complex feedstocks such as microalgal oil.

Selective Sequestration and Hydrogenation of Crude Microalgal Oil with AP-Ni-MSN. Rather than controlling the product selectivity of the reaction, the primary role of the amine groups in AP-Ni-MSN is the selective adsorption of FFA. This function is especially important when the material is used in the processing of complex feedstocks. Microalgal oil feedstock is typically rich in FFAs, containing mainly saturated C_{16} (50 wt %) and unsaturated C_{16} fatty acids (30 wt %).[52,53] As mentioned above, in biodiesel production, a refinery process is required to selectively remove these FFAs and make the feedstock suitable for processing. Thus, the AP-Ni-MSN based sequestration catalysis could be well integrated into the production chain of biodiesel, as it would remove the acidic FFAs that neutralize the transesterification catalyst and selectively upgrade the FFAs to diesel-range alkanes (Scheme 3).

To show the integration of this approach into the biodiesel production chain, we treated microalgal oil with AP-Ni-MSN. A hexane extract from microalgae was first analyzed by atmospheric pressure chemical ionization–high resolution mass spectrometry (APCI-HRMS) and GC-MS to establish the lipid composition and determine the amount of FFAs present. The chain length of FFAs detected in the microalgal extract ranged from C_{12} to C_{20}. The extract (10 mL) was then mixed with AP-Ni-MSN (10 mg) and set in a mechanical shaker for 6 h. After separation of the material from the supernatant, the latter was analyzed by APCI-HRMS. This technique revealed that the concentrations of triglycerides, diglycerides, terpenes, and sterols in the microalgal extract remained almost constant after sequestration of the FFAs with AP-Ni-MSN (Figure 8a,b). The AP-Ni-MSN containing the sequestered FFAs was subsequently hydrogenated under the same conditions used before for oleic acid. GC-MS analysis revealed that the AP-Ni-MSN sequestered up to 47 wt % of the FFAs in the microalgal extract and catalyzed the conversion of 66% of them into liquid hydrocarbons. The most abundant fatty acid in the original extract was C_{16}, and it was also the most sequestered FFA (68 wt %). *n*-Pentadecane was the major liquid hydrocarbon obtained, which presumably resulted from the decarbonylation of sequestered C_{16} FFAs (Figure 8c,d).

CONCLUSIONS

We introduced an integrated approach for the refinery of FFA-rich oils, in which adsorbent and catalytic sites were coimmobilized within the pores of a high surface support. The FFAs could be selectively removed from the oils by adsorbent amines and converted directly into hydrocarbons by catalytic Ni nanoparticles. The tethered organic groups affected the catalytic activity of the Ni nanoparticles toward the hydrogenation of FFAs, leading to less cracking and more hydrodeoxygenation than amine-free Ni-MSN. Saturating the AP-Ni-MSN material with FFAs prior to performing the hydrogenation reduced further the decarbonylation of the substrate, and consequently improved the carbon economy of the process. AP-Ni-MSN could be efficiently employed to sequester FFAs from crude microalgal oil and convert them into hydrocarbons with significant carbon economy. This sequestration-catalysis approach can be integrated to the refinery of FFA-rich renewable feedstocks to isolate and transform FFAs for biofuel production, leaving other valuable chemicals available for downstream processing.

Scheme 3. Pathways for the Production of Biofuels from FFA-Rich Feedstocks.[a,b,c]

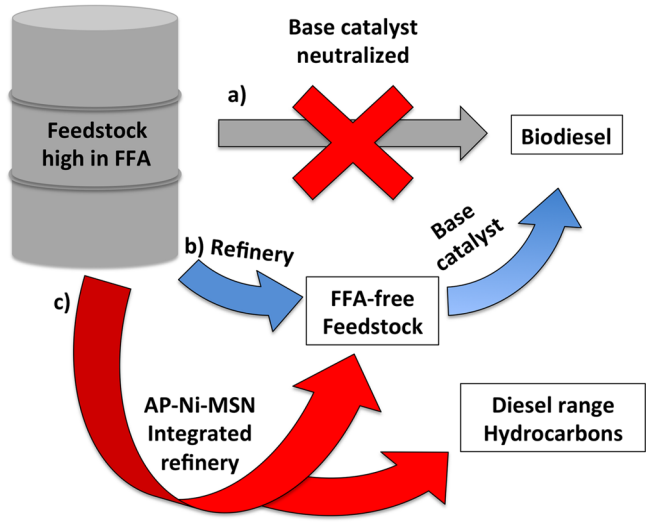

[a]Direct conversion is prevented when FFAs neutralize the catalyst. [b]FFA is removed before transesterification. [c]FFAs are sequestered with AP-Ni-MSN and hydrogenated to hydrocarbons, and the remaining feedstock is transesterified into biodiesel.

ASSOCIATED CONTENT

Supporting Information

Additional materials characterization, infrared spectra, product distribution plots at different amine loadings, and pore volume versus product distribution plots. This material is available free of charge via the Internet at http://pubs.acs.org.

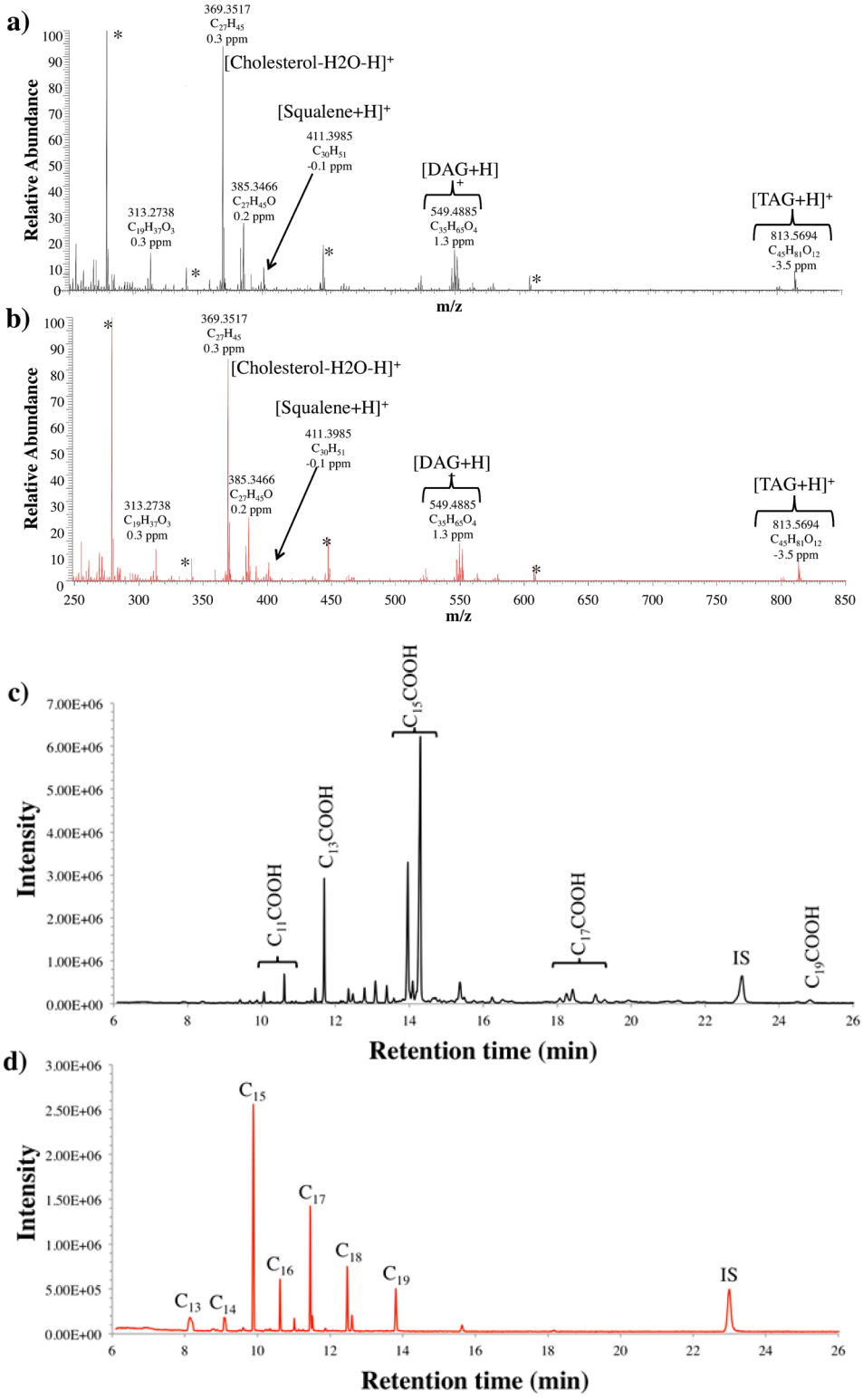

Figure 8. APCI-HRMS spectra of microalgal oil extract (a) before and (b) after mixing with AP-Ni-MSN. Solvent contamination peaks are designated with an asterisk (∗), and the peaks at *m*/*z* 313.2738 and 385.3466 are tentatively assigned as the methyl ester of ricinoleic acid and cholest-4-en-3-one, respectively. (c) FFA profile of microalgal extract and (d) hydrocarbon distribution resulting from the selective sequestration and catalytic processing of the FFAs with AP-Ni-MSN.

AUTHOR INFORMATION

Corresponding Author

*E-mail: islowing@iastate.edu.

Notes

The authors declare no competing financial interest.

ACKNOWLEDGMENTS

This research was supported at the Ames Laboratory by the U.S. Department of Energy, Office of Basic Energy Sciences. Ames Laboratory is operated for the U.S. Department of Energy by Iowa State University under contract no. DE-

AC02-07CH11358. C.F. would like to thank U.S. Department of Energy's Summer Undergraduate Internship Program (SULI) for the support to contribute to this research.

REFERENCES

(1) Atadashi, I. M.; Aroua, M. K.; Aziz, A. R. A.; Sulaiman, N. M. N. *Appl. Energy* **2011**, *88*, 4239−4251.
(2) Karaosmanoğlu, F.; Cığızoğlu, K. B.; Tüter, M.; Ertekin, S. *Energy Fuels* **1996**, *10*, 890−895.
(3) Al-Sabawi, M.; Chen, J.; Ng, S. *Energy Fuels* **2012**, *26*, 5355−5372.
(4) Lou, W.-Y.; Zong, M.-H.; Duan, Z.-Q. *Bioresour. Technol.* **2008**, *99*, 8752−8758.
(5) Yan, S.; Salley, S. O.; Ng, S. *Appl. Catal., A* **2009**, *353*, 203−212.
(6) Valenstein, J. S.; Kandel, K.; Melcher, F.; Slowing, I. I.; Lin, V. S. Y.; Trewyn, B. G. *ACS Appl. Mater. Interf.* **2012**, *4*, 1003−1009.
(7) Lee, Y.; Leverence, R.; Smith, E.; Valenstein, J.; Kandel, K.; Trewyn, B. *Lipids* **2013**, 1−9.
(8) Li, L.; Coppola, E.; Rine, J.; Miller, J. L.; Walker, D. *Energy Fuels* **2010**, *24*, 1305−1315.
(9) šimáček, P.; Kubička, D.; Šebor, G.; Pospíšil, M. *Fuel* **2009**, *88*, 456−460.
(10) Donnis, B.; Egeberg, R.; Blom, P.; Knudsen, K. *Top. Catal.* **2009**, *52*, 229−240.
(11) Petrus, L.; Noordermeer, M. A. *Green Chem.* **2006**, *8*, 861−867.
(12) Santana, R. C.; Do, P. T.; Santikunaporn, M.; Alvarez, W. E.; Taylor, J. D.; Sughrue, E. L.; Resasco, D. E. *Fuel* **2006**, *85*, 643−656.
(13) Lestari, S.; Simakova, I.; Tokarev, A.; Mäki-Arvela, P.; Eränen, K.; Murzin, D. *Catal. Lett.* **2008**, *122*, 247−251.
(14) Mäki-Arvela, P.; Kubickova, I.; Snåre, M.; Eränen, K.; Murzin, D. Y. *Energy Fuels* **2006**, *21*, 30−41.
(15) Snåre, M.; Kubičková, I.; Mäki-Arvela, P.; Eränen, K.; Murzin, D. Y. *Ind. Eng. Chem. Res.* **2006**, *45*, 5708−5715.
(16) Snåre, M.; Kubičková, I.; Mäki-Arvela, P.; Eränen, K.; Wärnå, J.; Murzin, D. Y. *Chem. Eng. J.* **2007**, *134*, 29−34.
(17) Lestari, S.; Mäki-Arvela, P. i.; Bernas, H.; Simakova, O.; Sjöholm, R.; Beltramini, J.; Lu, G. Q. M.; Myllyoja, J.; Simakova, I.; Murzin, D. Y. *Energy Fuels* **2009**, *23*, 3842−3845.
(18) Lestari, S.; Mäki-Arvela, P.; Simakova, I.; Beltramini, J.; Lu, G.; Murzin, D. *Catal. Lett.* **2009**, *130*, 48−51.
(19) Rozmysłowicz, B.; Mäki-Arvela, P.; Lestari, S.; Simakova, O.; Eränen, K.; Simakova, I.; Murzin, D.; Salmi, T. *Top. Catal.* **2010**, *53*, 1274−1277.
(20) Do, P.; Chiappero, M.; Lobban, L.; Resasco, D. *Catal. Lett.* **2009**, *130*, 9−18.
(21) Yang, Y.; Ochoa-Hernández, C.; de la Peña O'Shea, V. A.; Coronado, J. M.; Serrano, D. P. *ACS Catal.* **2012**, *2*, 592−598.
(22) Shiju, N. R.; Guliants, V. V. *Appl. Catal., A* **2009**, *356*, 1−17.
(23) Zhang, K.; Hu, X.; Liu, J.; Yin, J.-J.; Hou, S.; Wen, T.; He, W.; Ji, Y.; Guo, Y.; Wang, Q.; Wu, X. *Langmuir* **2011**, *27*, 2796−2803.
(24) Park, J. Y.; Zhang, Y.; Grass, M.; Zhang, T.; Somorjai, G. A. *Nano Lett.* **2008**, *8*, 673−677.
(25) Hou, W.; Dehm, N. A.; Scott, R. W. J. *J. Catal.* **2008**, *253*, 22−27.
(26) Paterson, J.; Potter, M.; Gianotti, E.; Raja, R. *Chem. Commun.* **2011**, *47*, 517−519.
(27) Kubička, D.; Kaluža, L. *Appl. Catal., A* **2010**, *372*, 199−208.
(28) Kubička, D.; Horáček, J. *Appl. Catal., A* **2011**, *394*, 9−17.
(29) Huber, G. W.; O'Connor, P.; Corma, A. *Appl. Catal., A* **2007**, *329*, 120−129.
(30) Viljava, T. R.; Komulainen, R. S.; Krause, A. O. I. *Catal. Today* **2000**, *60*, 83−92.
(31) Laurent, E.; Delmon, B. *J. Catal.* **1994**, *146*, 281−291.
(32) Crossley, S.; Faria, J.; Shen, M.; Resasco, D. E. *Science* **2010**, *327*, 68−72.
(33) Huang, Y.; Xu, S.; Lin, V. S. Y. *ChemCatChem.* **2011**, *3*, 690−694.
(34) Ide, Y.; Kagawa, N.; Sadakane, M.; Sano, T. *Chem. Commun.* **2012**, *48*, 5521−5523.
(35) Peng, B.; Yuan, X.; Zhao, C.; Lercher, J. A. *J. Am. Chem. Soc.* **2012**, *134*, 9400−9405.
(36) Peng, B.; Yao, Y.; Zhao, C.; Lercher, J. A. *Angew. Chem., Int. Ed.* **2012**, *51*, 2072−2075.
(37) Kim, T.-W.; Slowing, I. I.; Chung, P.-W.; Lin, V. S.-Y. *ACS Nano* **2010**, *5*, 360−366.
(38) Zhao, D.; Feng, J.; Huo, Q.; Melosh, N.; Fredrickson, G. H.; Chmelka, B. F.; Stucky, G. D. *Science* **1998**, *279*, 548−552.
(39) Richard-Plouet, M.; Guillot, M.; Vilminot, S.; Leuvrey, C.; Estournès, C.; Kurmoo, M. *Chem. Mater.* **2007**, *19*, 865−871.
(40) Wan, Y.; Zhao. *Chem. Rev.* **2007**, *107*, 2821−2860.
(41) Vradman, L.; Landau, M. V.; Kantorovich, D.; Koltypin, Y.; Gedanken, A. *Microporous Mesoporous Mater.* **2005**, *79*, 307−318.
(42) Rodrigues, C. E. C.; Meirelles, A. J. A. *J. Chem. Eng. Data* **2008**, *53*, 1698−1704.
(43) Dunford, N.; King, J. *J. Am. Oil Chem. Soc.* **2001**, *78*, 121−125.
(44) Liu, A. M.; Hidajat, K.; Kawi, S.; Zhao, D. Y. *Chem. Commun.* **2000**, *0*, 1145−1146.
(45) Mureseanu, M.; Reiss, A.; Stefanescu, I.; David, E.; Parvulescu, V.; Renard, G.; Hulea, V. *Chemosphere* **2008**, *73*, 1499−1504.
(46) Sharma, K. K.; Anan, A.; Buckley, R. P.; Ouellette, W.; Asefa, T. *J. Am. Chem. Soc.* **2008**, *130*, 218−228.
(47) Cooper, J. K.; Franco, A. M.; Gul, S.; Corrado, C.; Zhang, J. Z. *Langmuir* **2011**, *27*, 8486−8493.
(48) Davar, F.; Fereshteh, Z.; Salavati-Niasari, M. *J. Alloys Compd.* **2009**, *476*, 797−801.
(49) Prins, R. In *Advances in Catalysis*; Academic Press: New York, 2001; Vol. *46*, pp 399−464.
(50) Portefaix, J. L.; Cattenot, M.; Guerriche, M.; Thivolle-Cazat, J.; Breysse, M. *Catal. Today* **1991**, *10*, 473−487.
(51) Aguado, J.; Serrano, D. P.; Escola, J. M.; Briones, L. *Fuel* **2013**, *109*, 679−686.
(52) Van Vooren, G.; Le Grand, F.; Legrand, J.; Cuiné, S.; Peltier, G.; Pruvost, J. *Bioresour. Technol.* **2012**, *124*, 421−432.
(53) Olofsson, M.; Lamela, T.; Nilsson, E.; Bergé, J. P.; del Pino, V.; Uronen, P.; Legrand, C. *Energies* **2012**, *5*, 1577−1592.